高等学校化学学报
CHEMICAL JOURNAL OF CHINESE UNIVERSITIES
综合评述

环状聚合物的可规模化制备及功能化复合材料研究进展

屈开儒[1,2#], 郭绿洲[3#], 王文彬[4#], 颜徐州[4], 曹学正[3], 杨振忠[1]

(1. 清华大学化学工程系高分子研究所, 先进材料教育部重点实验室, 北京 100084;
2. 中石化(北京)化工研究院股份有限公司, 北京 100013;
3. 厦门大学物理科学与技术学院物理系, 福建省柔性功能材料重点实验室, 厦门 361005;
4. 上海交通大学化学生物协同物质创制全国重点实验室, 教育部变革性分子前沿科学中心, 化学化工学院, 上海 200240)

摘要 聚合物通常含有不同组成与数目的端基,其物理化学性质与此密切相关. 环状聚合物不含端基, 展现出独特的物理化学性能, 如更小的流体力学尺寸和延缓的降解速度, 引起人们广泛关注. 发展高效的合成方法, 实现环状聚合物的可规模化制备及组分与微结构的精准调控是高分子科学的前沿研究方向. 本文以动态单链纳米颗粒内环化方法可规模制备环状聚合物为例, 展示其面临的关键问题. 以小尺寸环状有机结构化合物为例, 展示了其在若干复合材料中的典型特性. 未来将更加聚焦发展高效合成方法, 精准控制环状聚合物尺寸、组成及序列结构, 为其规模制备和商业化及高性能复合材料的发展提供新范式.

关键词 环状聚合物; 规模制备; 单链纳米颗粒; 特性; 复合材料

中图分类号 O631.1 **文献标志码** A doi: 10.7503/cjcu20250212

Recent Progresses in Synthesis of Cyclic Polymers in Large-scale and Some Functionalized Composites

QU Kairu[1,2#], GUO Lyuzhou[3#], WANG Wenbin[4#], YAN Xuzhou[4], CAO Xuezheng[3], YANG Zhenzhong[1*]

(*1. Institute of Polymer Science and Materials, Department of Chemical Engineering, Key Laboratory of Advanced Materials of Ministry of Education, Tsinghua University, Beijing* 100084, *China*;
2. SINOPEC(Beijing) Research Institute of Chemical Industry Co. Ltd, Beijing 100013, *China*;
3. Department of Physics, Fujian Provincial Key Laboratory for Soft Functional Materials Research, College of Physical Science and Technology, Xiamen University, Xiamen 361005, *China*;
4. State Key Laboratory of Synergistic Chem-Bio Synthesis, Frontiers Science Center for Transformative Molecules of Ministry of Education, School of Chemistry and Chemical Engineering, Shanghai Jiao Tong University, Shanghai 200240, *China*)

Abstract Among various architectures of polymers, end-group-free rings have attracted growing interests due to their distinct physicochemical performances over the linear counterparts which are exemplified by reduced hydrodynamic size and slower degradation. It is key to develop facile methods to large-scale synthesis of polymer rings

收稿日期: 2025-07-30. 网络首发日期: 2025-09-16.
联系人简介: 杨振忠, 男, 博士, 教授, 主要从事功能空间精准分区、微纳结构精细可控的多组分高分子复合体系方面的研究.
E-mail: yangzhenzhong@tsinghua.edu.cn
基金项目: 国家自然科学基金(批准号: 52293472, 22473096 和 22471164)资助.
Supported by the National Natural Science Foundation of China(Nos.52293472, 22473096 and 22471164).
共同第一作者.

with tunable compositions and microstructures. Recent progresses in large-scale synthesis of polymer rings against single-chain dynamic nanoparticles, and the example applications in synchronous enhancing toughness and strength of polymer nanocomposites are summarized. Once there is the breakthrough in rational design and effective large-scale synthesis of polymer rings and their functional derivatives, a family of cyclic functional hybrids would be available, thus providing a new paradigm in developing polymer science and engineering.

Keywords Cyclic polymer; Large-scale synthesis; Single-chain nanoparticle; Performance; Composite

1 Introduction

Conventional polymer chains contain diverse end groups which exhibit significant impacts on physical properties such as glass transition behavior, crystallinity and viscoelasticity[1]. In comparison, cyclic polymers (or rings) without end groups display superior performances, including reduced melt viscosity[2], smaller hydrodynamic size[3], higher glass transition temperature and crystallinity[4—6]. The cyclic polymers are more promising in such as biomedicine[7,8] and optoelectronics[9]. As an example, a cyclic polymer coating can more effectively suppress nonspecific protein adsorption[10]. In a gel network, cyclic polymers act as dynamic cross-linkers, resulting in a higher elastic modulus and mechanical stability[11]. Cyclic poly(ethylene glycol) (PEG)-coated Au NP becomes more stable against aggregation under thermal and solvent variations[12]. The cyclic polymers without chain-end steric hindrance can self-assemble into more compact core-shell micelles. Cyclic polymers are superior in enhancing thermal resistance and ionic stress since inter-micellar bridging and entanglement from the chain ends are absent. Conventionally, multiple analytical techniques including gel permeation chromatography(GPC), analytical ultracentrifugation(AUC), nuclear magnetic resonance(NMR) spectroscopy, and light scattering measurements[13—16] are combined to differentiate between linear precursors, intramolecular ring closure, and intermolecular coupling products. Each technique provides the corresponding specific aspects. The information on molecular weight and distribution and hydrodynamic volume by GPC yields indicates that one cyclic polymer exhibits a longer retention time than the linear precursor. The accurate molecular weight and sedimentation coefficient could be measured by AUC. A cyclic structure should display a higher sedimentation coefficient. NMR offers the information on atomic-level structural and connectivity details. And light scattering methods provide the information on absolute molecular weight and topological parameters. The combinational characterization provides a comprehensive analysis to distinguish cyclic and linear polymer architectures. However, extensive exploration of the unique performances of cyclic polymers in practical applications remains highly restricted by the lack of effective methods to synthesize a large quantity of pure polymer rings[17—21].

2 Recent Advances in Large-scale Synthesis of Polymer Rings

Since the first identification of biomacromolecular cyclic topologies in 1960s, development of effective synthetic methods to large-scale fabrication of polymer rings has gained growing interest[22,23]. The conventional "ring-chain" equilibrium method inevitably yields impurities of high molecular weights[24]. The classical synthetic methods are essentially classified into two categories of ring-closure and ring-expansion(Fig.1). The historical advances in synthesis of polymer rings and the characteristics have been comprehensively surveyed in a series of review papers[25—29]. The former method involves the continuous inserting of monomers into the cyclic catalysts to achieve the rings after the polymerization[30,31]. Although high-molecular-weight polymer rings could be synthesized at a relatively high concentration, the method is highly restricted for specific monomers and cyclic catalysts. And the polymerization lacks precision control with a broad molecular weight distribution and multi-cycle impurities coexistent. In comparison, the ring-closure method offers superior compatibility with

the advanced polymerization techniques including atom transfer radical polymerization (ATRP), reversible addition-fragmentation chain transfer polymerization (RAFT) and living anionic polymerization[32,33]. In principle, precision synthesis of cyclic architectures becomes feasible since a family of well-defined telechelic polymers and efficient cyclization reactions are readily available. In practice, the method is valid for those polymers of appropriate molecular weights ($\overline{M}_w$) below 25000, which could be well rationalized by classical Jacobson-Stockmayer theory[34]. Otherwise, the end groups would be separated too far to contact for the effective closure. What's more, tedious separation of catalysts after the cyclization makes the method less attractive[35]. Development of facile methods for the large-scale synthesis of polymer rings in concentrated solutions remains challenging, and further exploration of unique performances of polymer rings and practical applications are severely delayed.

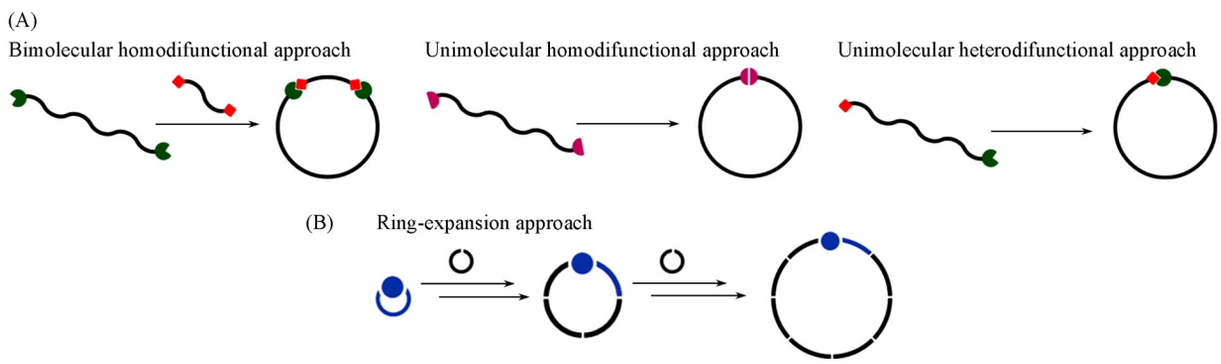

Fig. 1 Schematic ring closure method to prepare cyclic polymers *via* three representative strategies(A) and the ring-expansion strategy(B)[28]

(A) A_2+B_2 bimolecular coupling, A_2 unimolecular self-cyclization, A-B unimolecular self-cyclization.
Copyright 2009, the Royal Society of Chemistry.

2.1 Coupling Reactions

Traditional synthesis of cyclic polymers of high molecular weights *via* ring-closure should be conducted under dilution conditions in order to suppress intermolecular reactions. Since Rempp *et al.*[36] reported the synthesis of cyclic polystyrene *via* coupling di-functional living PS chains (achieved by anionic polymerization) with dibromo-*p*-xylene, it has been proved that various linkers are effective to achieve the coupling[37—41]. Although a family of cyclic polymers of high molecular weights have been synthesized, the cyclization is usually inefficient below 50%. And a tedious separation is involved in order to achieve pure cyclic polymers.

Significant increment of cyclization yield is crucial in development of highly efficient coupling methodologies for ring-closure. Tillman *et al.*[42] developed a radical trap-assisted atom transfer radical coupling (RTA-ATRC) with nitrosobenzene to generate telechelic poly(methyl methacrylate) (PMMA) with radical terminal ends. The cyclization was performed by radical coupling at a concentration of 7 mg/mL. Tezuka *et al.*[43] proposed a novel zwitterionic approach to prepare telechelic polystyrene (PS) and poly(tetrahydrofuran) [poly(THF)] with complementary cyclic ammonium and carboxylate groups at the opposite ends, and further achieve the efficient ring closure by subsequent electrostatics driven self-assembly and covalent bonding. The end groups approach at a closer proximity after the electrostatics-assisted pre-organization, and the covalent coupling efficiency is significantly improved. The representative reactions of Williamson etherification[44] and double strain-promoted azide-alkyne clicking (DSPAAC) are proved applicable for the ring-closure (Fig. 2)[45,46]. The coupling reactions are valid for bi-molecular cyclization, offering the kinetic and thermodynamic merits to improve cyclization efficiency at a higher concentration.

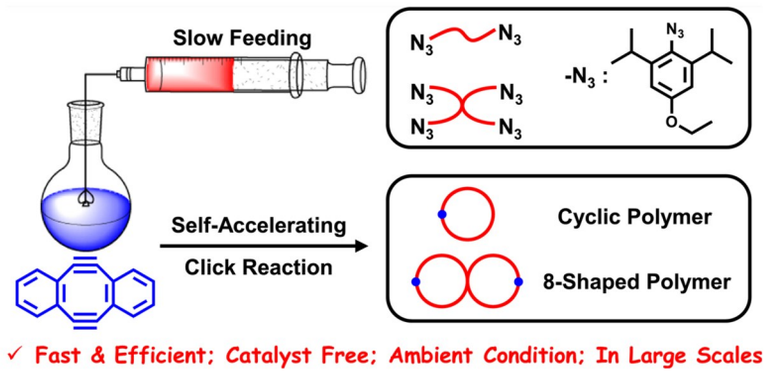

Fig. 2 Double strain-promoted azide-alkyne clicking toward the efficient ring-closure reactions[45]

Copyright 2020, American Chemical Society.

2.2 Circulatory Cyclization Strategy

Conventional ring-closure should be performed under ultra-dilute conditions with a low yield inherently. In order to break this restriction, continuous-flow technique was proposed to increase cyclization efficiency in a final concentrated solution. Zhu *et al.*[47] reported an evaporation-condensation-extraction-inflow strategy for the Cu-catalyzed azide/alkyne cycloaddition (CuAAC), enabling the gram-scale synthesis of cyclic polystyrene (PS) and poly(methyl methacrylate) (PMMA) (Fig. 3). The linear precursor was injected at an extremely low concentration. After the cyclization and evaporation of the solvent, the cyclic product was separated by precipitation while the linear polymer remained soluble. It is noted that the circulatory cyclization could continuously proceed until all the batched linear polymers were completely consumed. Zhang *et al.*[48] proposed a smart method by light-induced cyclization between thiocarbonyl and salicylaldehyde moieties at the linear PS to achieve the cyclic polymer at a gram-scale. This method could be further extended by incorporating a solvent circulation system to lower solvent consumption[49]. Along with the continuous-flow routine, [2+2] photocycloaddition was performed on styrylpyrene terminated polymers [PS, polyethylene oxide (PEO), poly-ε-caprolactone (PCL)] to achieve scalable production of the corresponding cyclic polymers at a rate of 54 mg/h[50]. Similarly, the Glaser coupling was used in a micro-reaction system toward efficient synthesis of cyclic polymers[51]. Although continuous-flow represents a substantially intensified progress, the strategy essentially follows the dilute guideline in order to ensure the efficient intramolecular cyclization.

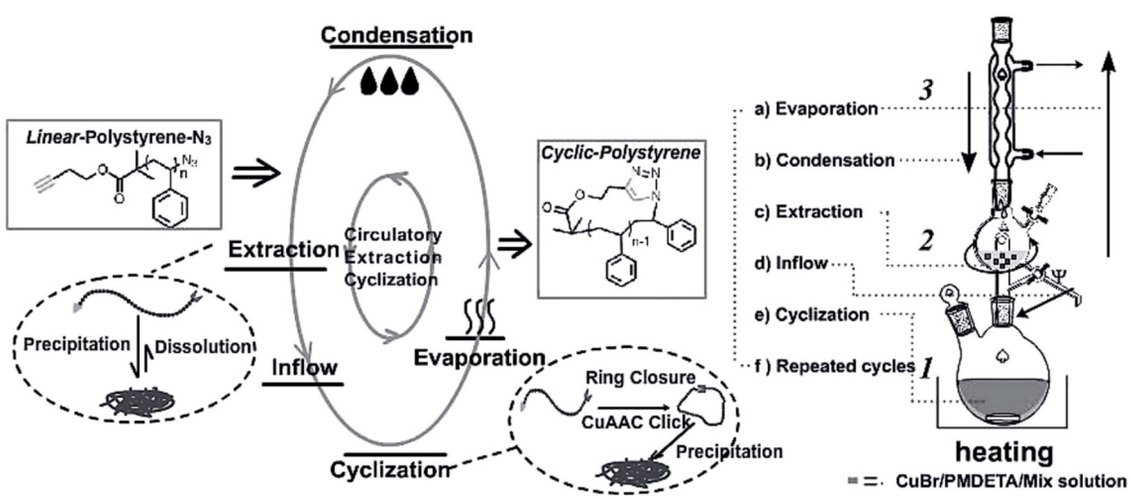

Fig. 3 Schemes of the reaction and equipment to synthesize cyclic polymers by ATRP-CuAAC cyclization *via* the evaporation/condensation/extraction/inflow process[47]

Copyright 2013, John Wiley and Sons.

2.3 Solvation Strategy

Rational manipulation of solvation of polymers enables precision control of their aggregation, thus increasing the cyclization efficiency. In the case of α-alkyne and ω-azide terminated poly(2-alkyl-2-oxazoline) copolymers[52], increment of the hydrophilicity is conducive to solvation of the polymer to achieve a high cyclization yield of 86% at a high concentration of 3 mg/mL. Liu *et al.*[53] developed a micelle-unimolecule equilibrium strategy of α-alkyne and ω-azide terminated POEGMA based diblock copolymer to achieve the "selective" intramolecular "click" ring closure (Fig.4). While the block of PEO_2GMA is responsible for forming the core with the azide groups embedded thus protected inwardly at an appropriate temperature, the block of PEO_9GMA is responsible for stabilizing the micelle at the corona with the alkyne groups positioned at the exterior surface. It is noted that the ring-closure should be conducted slowly. It remains challenging to achieve much higher efficient ring-closure at a much higher concentration toward large-scale synthesis of pure polymer rings.

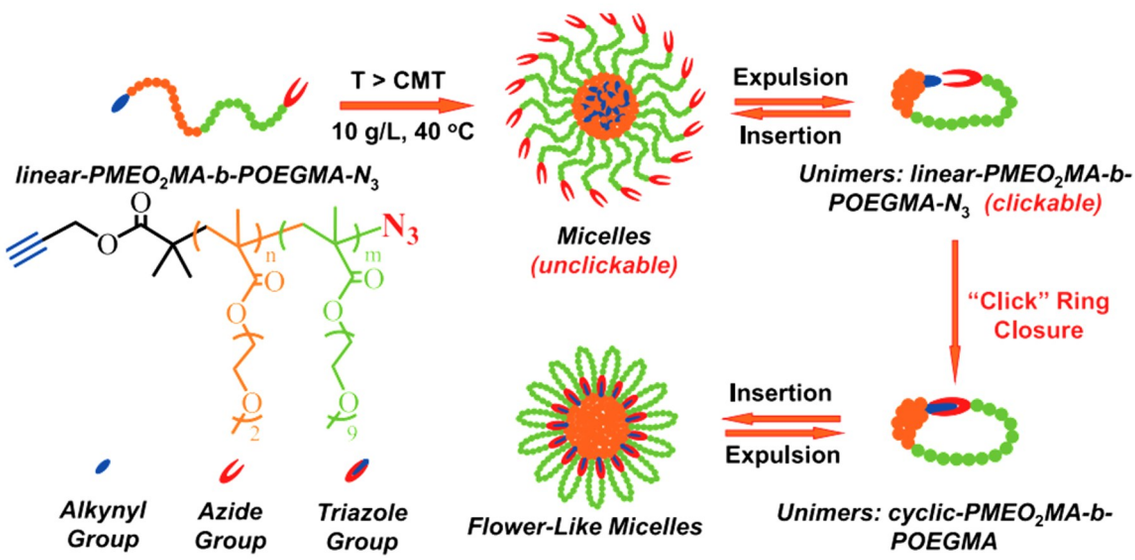

Fig. 4 Schematic preparation of copolymer rings by combinational supramolecular self-assembly and "selective" intramolecular "click" ring closure[53]

Copyright 2009, American Chemical Society.

2.4 Single-chain Nanoparticle Confined Couplings

Natural species including highly charged polymers such as DNA and RNA are self-assembled in corresponding confined cargos such as viral capsids and cells to perform biological functions[54]. Inspired by these compact hierarchical structures, it is anticipated that polymer rings could be effectively synthesized under such crowded conditions. Hong *et al.*[55—57] reported the cyclization of an example polymer of anthracene terminated poly{[oligo(ethylene glycol) acrylate]-co-(dodecyl acrylate)}[P(OEGA-co-DDA)] within the self-folding single chain nanoparticles. In an aqueous solution, the linear polymer can spontaneously fold into a single-chain nanoparticle (SCNP) at a relatively high concentration (40—90 mg/mL) depending on the OEGA/DDA molar ratio. While the PDDA segment is responsible for forming the core by hydrophobic association, the POEGA segment is responsible for stabilizing the SCNP by hydrogen bonding with water. Upon UV irradiation, the anthracene groups at the ends are cyclized to achieve the ring closure. This approach relies on stringent control of composition and architecture of the polymers for the effective self-folding of single-chains. At a higher concentration, intermolecular aggregates of multi-chains may coexist with the SCNPs, and the exclusive intramolecular ring closure at the SCNP will fail.

Alternatively, Yang *et al.*[58] proposed a robust strategy for large-scale synthesis of highly pure polymer

rings *via* electrostatics-mediated ring-closure at the dynamic SCNPs in more concentrated solutions (Fig.5). The strategy is universal for a range of polymers and ring-closure chemistries. For example, in poly[2-(dimethylamino)ethyl methacrylate](PDMAEMA) based random and block copolymers, the dynamic SCNPs can be effectively formed within minutes by the electrostatics-mediated intramolecular crosslinking at an unprecedentedly high concentration above 200 mg/mL. When salicylaldehyde and dithioester groups are terminated at the telechelic PDMAEMA chains, the coupling can be completely achieved at the dynamic SCNP within 10 min under UV irradiation at 365 nm at a high concentration of 150 mg/mL. It is noted that the ring closure is exclusively in the intramolecular mode, and no intermolecularly crosslinked byproducts are detected. After elimination of the acids from the dynamic SCNPs with $NaHCO_3$, pure polymer rings were obtained. The ring-shape could be visualized under TEM after extending the ring *via* grafting PEO-NCO with hydroxyl-groups onto the ring[Fig.5(B)]. In comparison, the linear polymer chain displays the shape of nanowire under TEM upon the chain extension[Fig.5(C)]. Poly(2-(dimethylamino) ethyl methacrylate)-co-poly(pentafluorophenyl methacrylate) and poly(phenyl methacrylate)-block-poly[2-(dimethylamino) ethyl methacrylate]-co-poly(pentafluorophenyl methacrylate)-block-poly(phenyl methacrylate) were used as the example random and block copolymers to derive the corresponding polymer rings with tunable compositions and microstructures. In order to demonstrate the generality of the method, thiol-ene terminated telechelic PDMAEMA chains were used for large-scale synthesis of polymer rings by UV initiation at 415 nm in the presence of catalytic diphenyl(2,4,6-trimethylbenzoyl)phosphine oxide(TPO). The electrostatics-mediated ring closure at dynamic SCNPs is highly advantageous in easy processing at higher solid content, higher conversion rate, and nearly 100% purity. This method paves the avenue to providing sufficient amount of pure polymer rings with tunable compositions and microstructures, and enables extensive exploration of their unique performances for practical applications. Similarly, another exemplary functional copolymer of poly(pentafluorophenyl methacrylate)-block-poly[2-(dimethylamino)ethyl methacrylate]-block-poly(pentafluorophenyl methacrylate) was synthesized by RAFT polymerization, and AIEgens and styryl groups were further grafted onto the end blocks by reactions

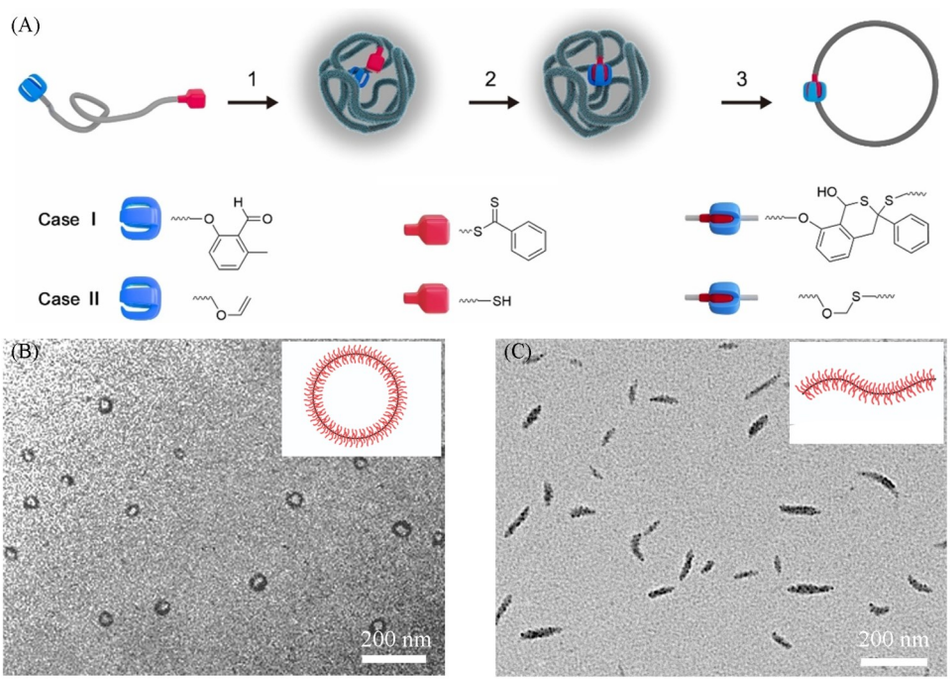

Fig. 5 Electrostatics-mediated ring closure at the dynamic SCNP toward large-scale synthesis of pure polymer rings(A) and TEM images of the ring(B) and linear(C) polymer upon the chain extension[58]

with 1-(4-aminophenyl)-1, 2, 2-triphenylethene and 4-vinylaniline. The electrostatics-mediated ring-closure at the dynamic SCNP was successfully achieved at 50 mg/mL, which is inaccessible for the conventional ring closure methods. As a result, the AIEgen-functionalized polymer ring gives rise to a bright monochromic fluorescence at 417 nm, originating from individual compact AIEgen clusters on the ring. In comparison, the aggregates formed after intermolecular crosslinking exhibit additional emission at 480 nm from the coupled clusters. The unique AIE behavior of polymer rings offers a direct and sensitive method to discriminate intramolecular ring-closure and intermolecular crosslinking.

3 Properties of Polymer Rings

Polymer rings exhibit superior physicochemical properties over the linear counterparts owing to the closed-loop topologies. The covalent linkage of chain ends into a circular architecture eliminates the terminal groups and manifests profound effects on macroscopic performances at multi-scales[25]. In biomedical applications, ring polymers exhibit unique diffusion behavior that holds great promises in drug delivery and DNA/RNA genetic encoding and expression. The construction of thermodynamic models based on intermolecular interactions enables to quantitatively describe the energy change during the drug-ring polymer complexation, providing a guidance to enhance stability of the complexes and their compatibility with physiological environments[59]. The self-assemblies between ring polymers and drug molecules are highly promising for delivering drugs and genes[60—62].

3.1 Thermal Properties

The segmental dynamics and molecular interactions of polymer rings are significantly different, leading to distinct thermal behavior[63]. The poly(vinyl ether) based polymer ring was synthesized by cationic ring-opening polymerization by using a hemiacetal ester-based cyclic initiator[64]. As expected, the polymer ring exhibits a notably higher glass transition temperature(T_g, ℃)(Fig. 6), which originates from the reduced free volume. And the polymer rings display higher crystallization temperatures (T_c, ℃) and melting points(T_m, ℃)[65].

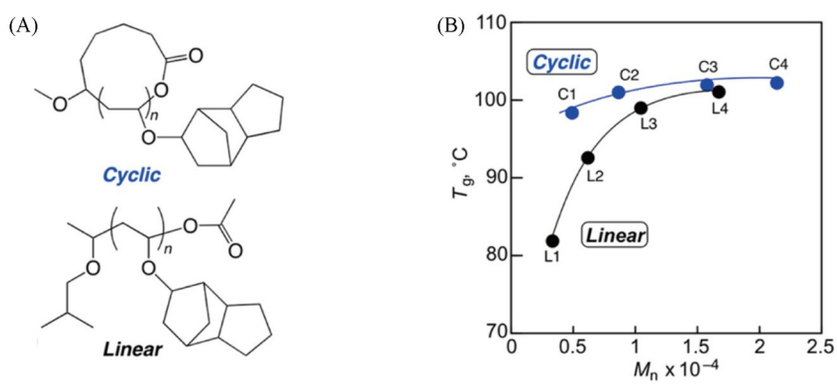

Fig. 6 Structures(A) and glass transition temperatures(B) of poly(vinyl ether) based rings and linear chains of varied molecular weights[64]

Copyright 2017, American Chemical Society.

3.2 Rheological Properties

Intrinsic viscosity and relaxation dynamics of polymer rings are greatly different from their linear counterparts[3]. A trace amount of polymer rings could result in a dramatically increased viscosity in polymer melts by the "threading" effect, where the linear chains penetrate the polymer rings to form an additional entangled network[66]. A series of high-purity cyclic polystyrene(C-PS) samples with varied molecular weights ($\overline{M}_n$=16000—370000) was synthesized by the ring-closure reactions and subsequent careful purification by

liquid chromatography[67]. It is shown that the intrinsic viscosity of C-PS ($[\eta]_C$) is substantially lower than that of its linear counterparts (L-PS, $[\eta]_L$), with an $[\eta]_C/[\eta]_L$ ratio of 0.57—0.63 which is also dependent on molecular weight [Fig. 7(A)]. The lower intrinsic viscosity is understandable due to the reduced chain entanglement.

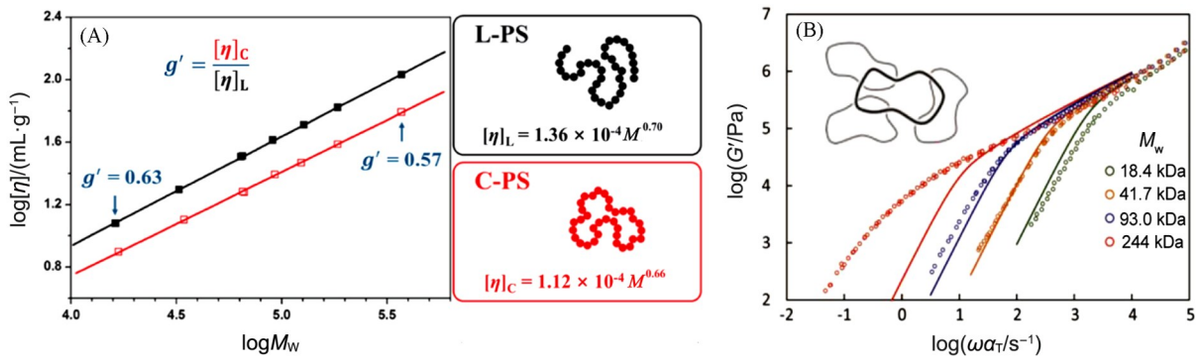

Fig. 7 The intrinsic viscosity([η], A)[67] and rouse model(solid lines) predicating storage modulus(G') of polystyrene rings, and the experimental data(open circles) at a reference temperature of 160 ℃(B)[68]

(A) Copyright 2017, American Chemical Society; (B) Copyright 2015, American Chemical Society.

The rubbery plateau in stress relaxation spectra disappears since the free chain ends are absent in the polymer rings with a significantly lower entanglement density [Fig.7(B)]. The relaxation behavior dependence on molecular weight indicates that the relaxations are more hindered at higher molecular weights[68—70]. Multi-scale simulations of polystyrene rings reveal that the terminal relaxation is accelerated with the rubbery plateau diminished. It is found that entanglement length of the polymer rings is approximately twice that of the linear chains[71]. Both the theoretical and experimental results reveal that the polymer rings display a rather weaker shear thinning behavior with an exponent parameter of 0.57 than the linear polymers with an exponent parameter of 0.89. Scaling theory further elucidates that polymer rings demonstrate a lower zero-shear viscosity[72]. For sufficiently large polymer rings, threading by other polymer chains into the closed cavity is allowed to generate unique clusters in the polymer alloys[73]. The resultant topological constraints give rise to restricted relaxation dynamics and complicated rheological behavior[74—76]. Simulation results indicate that the threading results in remarkably increased melt viscosity and mechanical toughness[77—79]. While polymer rings and linear chains exhibit comparable Rouse dynamics at short timescales, polymer rings are capable of suppressing non-Gaussian behavior at longer timescales, displaying a spatially homogeneous segmental dynamics by inter-ring cooperativity[80]. Rigid polymer rings demonstrate an anomalous rotational diffusion in melts. The rheological analyses reveal that polymer rings impart a frequency-dependent viscoelastic response with a higher viscosity at an elevated frequency, providing fundamental guidelines to design strong and tough polymer materials[81,82]. Rubinstein *et al.* proposed a comprehensive theoretical framework based on affine and phantom network models to well describe the mechanical response and rheology of polymer ring enhanced melts[83,84]. The closed-loop topology of polymer rings endows unique rheological properties to design and fabricate high performance polymer materials.

3.3 Self-assembly and Phase Behaviors

Cyclic polymers, as the end-free closed-loop architectures, own the distinctive topological constraints to govern the mobility of chain segments, thus regulating their thermodynamic characteristics and inducing remarkable size reduction and structural alteration during self-assembly. As a result, unique phase structures that are inaccessible to their linear counterparts are formed. In the example polystyrene-block-polyisoprene (PS-PI) based copolymers, while the linear PS-PI forms the "classical" spherical micelle as predicated by the

morphological parameters, the cyclic polymer is capable of assembling into a giant wormlike structure through the "sunflower-like" micelle intermediates[85]. In the case of poly(butyl acrylate)-b-poly(ethylene oxide)-b-poly(butyl acrylate) based triblock copolymers, the micelle of cyclic polymer demonstrates an enhanced thermal stability although spherical micelles of 20 nm in diameter are formed from both the polymers[86]. In the bulk thin-film self-assembled from the cyclic polystyrene-block-poly(ethylene oxide), the domain spacing is decreased by approximately 30% compared with the linear polymer film[87]. The remarkable reduction in domain size is inaccessible by simple decreasing the chain length in the conventional linear polymers. This finding demonstrates the merit of cyclic topology in constructing smaller patterns by self-assembly.

4 Effects of Polymer Rings in Nanocomposites

4.1 Polymer Rings

The conformational versatility of cyclic topologies under mechanical stress is manifested by flipping, twisting, and dynamic rearrangements, resulting in efficient energy dissipation and enhanced ductility[88]. A norbornene-based ring-opening metathesis was conducted to synthesize the copolymer, which was further functionalized with 120° dipyridyl ligands[89]. The metallacycle crosslinked polymers were constructed by subsequent self-assembly with either 60° or 120° Pt(II) acceptors [Figs. 8(A) and (B)]. A small amount (0.28%, molar fraction) of the dipyridyl side-chains on the macrocyclic crosslinkers leads to a substantial enhancement of mechanical performance. The polymer exhibits a high tensile strength of 20 MPa and a Young's modulus of 600 MPa and an exceptional toughness over 150 MJ/m^3. The metallacycle crosslinkers demonstrate controllable reversible deconstruction and reformation upon sequential treatment with tetrabutylammonium bromide and silver triflate, highlighting the outstanding stimuli-responsive nature of the materials. Similarly, incorporation of dibenzo-24-crown-8(DB24C8) macrocycles into the polymer backbone affords a cyclic-monomer constructed elastomer network (CCN) of an extraordinary toughness [Fig. 8(C)][90]. Copolymerization of

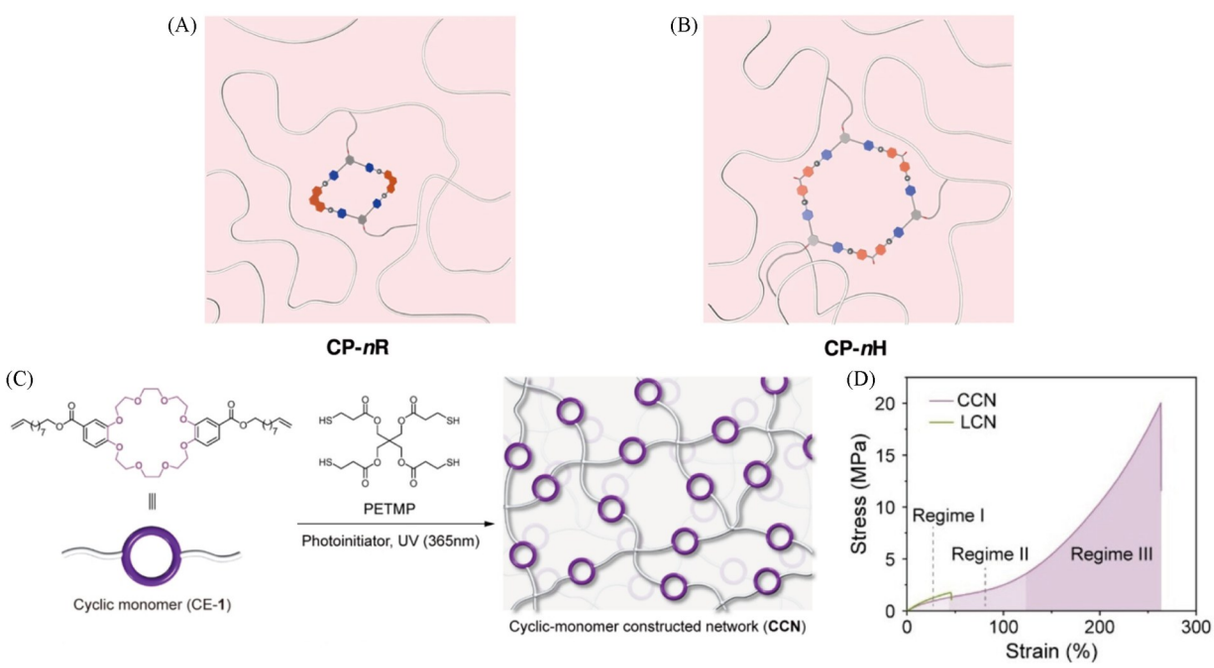

Fig. 8 Schematic illustration of the rhombic metallacycle crosslinked polymer network(CP-*n*R) formed using 60° Pt(II) acceptors(A) and the hexagonal metallacycle crosslinked polymer network(CP-*n*H) obtained with 120° Pt(II) acceptors(B)[89], schematic formation of CCN(C) and stress-strain profiles of LCN and CCN at a deformation rate of 100 mm/min(D)[90]

(A, B) Copyright 2024, Springer Nature; (C, D) Copyright 2024, John Wiley and Sons.

DB24C8 monomer with a tetra-armed crosslinker endows the network strands with the crown ether motif. The CCN exhibits greatly improved extensibility and strength. The CCN demonstrates 66-folds toughness compared to the linear counterpart[Fig.8(D)]. The stress-induced conformational transition of the DB24C8 macrocycles promotes synergistic energy dissipation and entropy driven toughening. The distinct binding affinities of DB24C8 toward various guest species such as potassium ions and secondary ammonium salts enable precise modulation of the elasticity and stimuli-responsive behavior.

4.2 Ring-chain Threading Structures

The ring-chain threading architecture constitutes a distinctive topological motif at both molecular and supramolecular scales, which could be extensively derived from macrocyclic host molecules including crown ethers, cyclodextrins, calix[*n*]arenes, pillar[*n*]arenes, and cucurbit[*n*]urils[91]. This paradigm is epitomized by pseudorotaxane and rotaxane complexes with a macrocyclic host threading onto a linear guest molecular axle, where sliding and rotation are permitted. In order to inhibit the dethreading, bulky stopper groups are appended at the axle ends to convert the pseudorotaxane into a mechanically interlocked yet stable rotaxane. When integrated as dynamic functional moieties in polymer networks, the rotaxane/pseudorotaxane units enable precise modulation of mechanical strength, toughness, and dynamic responsive behavior[92,93].

A complex between perfluorophenyl(5FBVI) and substituted phenyl(RBVI) was used as the guest to interact with the cucurbit[8]uril(CB[8]) macrocyclic host[94]. An exquisite control over dissociation of the dynamic crosslinking was achieved by adjusting the hydrophobic environment of the secondary RBVI phenyl group. The resultant glass-like supramolecular network exhibits a remarkable compressive resilience while the structural integrity is well retained after 12 cycles of compression and relaxation at 93% of strain. A maximum compressive strength of 100 MPa was achieved without fracturing. Fast self-healing could be achieved within 120 s at ambient temperature, which is originated from the dynamic sacrificial bonding and quasi-permanent crosslinking. The H_2G_2-type monomer consisting of two benzo-21-crown-7(B21C7, H_2) macrocyclic hosts and two diammonium(G_2) guest moieties were synthesized for the dynamic interaction(Fig. 9)[95]. The complementary host-guest recognition between B21C7 and ammonium groups gives rise to the [2]pseudorotaxane crosslinking, forming a self-crosslinkable supramolecular polymer network(SPN). The SPN is dynamic and reversible in both solution and gel, which originates from the profoundly temperature and pH triggered dissociation and reorganization. The network becomes activated at elevated temperature to accelerate the stress relaxation, making processing and modulation of the materials easier.

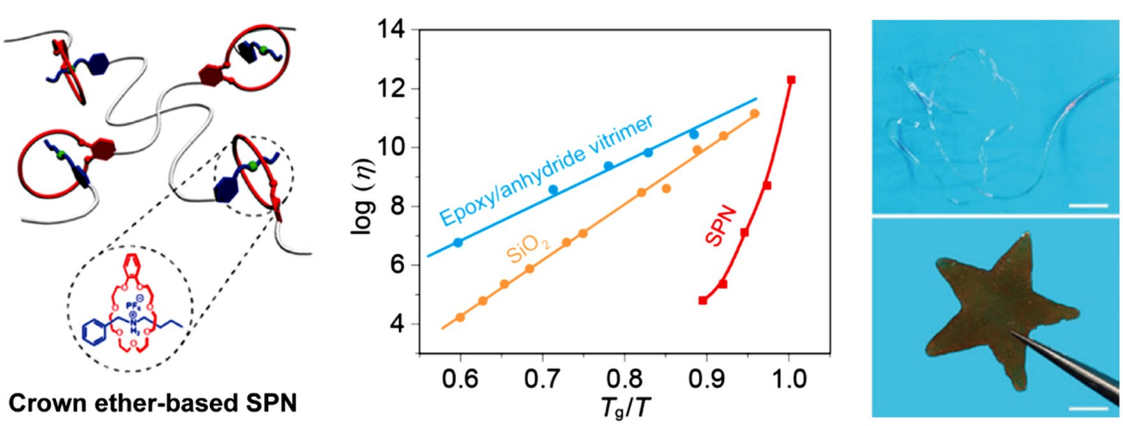

Fig. 9 A self-crosslinked supramolecular polymer network of easier processibility and moldability[95]

Copyright 2020, American Chemical Society.

Incorporation of a small molar fraction(≤0.5%) of [2]rotaxane crosslinker could attain a simultaneous enhancement of strength and toughness of the polymer network[Fig. 10(A)][96]. A macromolecular [2]rotaxane

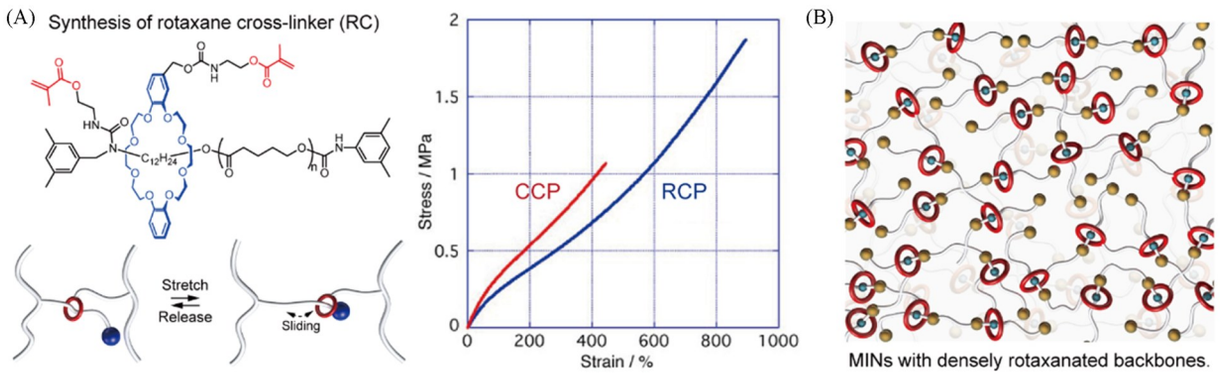

Fig. 10 Molecular architecture and dynamic behavior of the macromolecular [2]rotaxane crosslinker, and the mechanical performances of RCP and CCP(A)[96] and mechanical interlocking network with a densely rotaxanated backbone(B)[97]

(A) Copyright 2015, American Chemical Society; (B) Copyright 2022, Springer Nature.

crosslinker (RC) was synthesized from a polyester axle with two vinyl— groups capped. Radical polymerization of *n*-butyl acrylate in the presence of RC afforded the rotaxane crosslinked polymer (RCP), while the covalently crosslinked polymer (CCP) in the absence of RC served as the control to delineate the distinct effect of mechanical interlocking *versus* conventional covalent crosslinking. The RCP exhibits a much higher fracture stress and strain than the CCP which is attributed to the improved network homogeneity and mobility by the rotaxane crosslinking. A well-defined difunctional [2] rotaxane monomer bearing vinyl— groups at the macrocycle and axle was synthesized[97]. A mechanically interlocked network (MIN) with [2] rotaxane was achieved by photoinitiated thiol-ene click chemistry between 3,6-dioxa-1,8-octanedithiol (DODT) and pentaerythritol tetrakis(3-mercaptopropionate) (PETMP) [Fig.10(B)]. Both rheological characterization and molecular dynamics simulation reveal a sequential energy dissipation routine from chain orientation to dissociation of the host-guest interaction, to macrocycle sliding along the axle, and ultimate chain stretching once the macrocycle is driven to move toward the stopper group. This unique energy dissipation could be greatly intensified by incorporating MIN within the network to achieve the corresponding exceptional enhancements in extensibility, stiffness, toughness, and strength. A type of slide-ring materials (SRMs) were synthesized by threading poly(ethylene glycol) (PEG) chains across the α-cyclodextrin (CD) macrocycles with bulky end groups, in which CDs are freely sliding along the backbone akin to pulleys on a rope[98,99]. These CD rings are crosslinked in the shape of figure-of-eight, and the resultant steric hindrance from the end groups is responsible to preventing the dissociation unless the covalent bonding is cleaved. As a result, the network is much more stable alongside the unique mobility over the conventional chemical crosslinking. While the conventional covalently crosslinked gels are prone to chain scission after stress concentration, sliding of polymer chains by the macrocycles results in cooperative stress dissipation *via* mitigating damage. A novel entropy driven elasticity termed "sliding elasticity" is originated from inhomogeneous distribution of the mobile CDs which is weakly dependent on crosslinking density at low frequencies. This new performance is inaccessible in traditional networks whose elasticity is originated from conformational entropy which is highly dependent on crosslinking density. CD sliding is much slower with a much longer dynamic timescale than PEG segmental motion[100], indicating that the polymer deformation is capable of outpacing the pulley-mediated relaxation. The viscoelastic response of the slide-ring gels is featured with a characteristic "sliding state" at longer timescales or elevated temperatures which is corresponded to the rubbery plateau[101]. The unique sliding elasticity significantly alleviates stress concentration, thus governing recovery and strain resistance of the materials.

Multicyclic polydimethylsiloxanes(mc-PDMS) with controlled cyclic unit numbers and sizes were synthesized

via cyclopolymerization of α,ω-norbornene-terminated macromonomers[102]. mc-PDMS was effectively fixated within the network by subsequent *in-situ* crosslinking of silanol terminated PDMS with the tetrafunctional crosslinker. The trapping efficiency of mc-PDMS (above 80%) is much higher than that of the monocyclic PDMS (1c-PDMS), which is well maintained even when the mc-PDMS ring is smaller than the PDMS entanglement molecular weight (M_e). This phenomenon is confirmed by fluorescence imaging of the pyrene-dyed mc-PDMS. The higher the number-average molecular weight ($\overline{M}_n$) is, the higher the topological trapping efficiency will be. This characteristic is unattainable with single-ring polymers. The network is capable of incorporating mc-PDMS up to 50% (mass fraction). The multicyclic polymers serve as dynamic crosslinkers akin to molecular pulleys. Simulations reveal that smaller cyclic units at the multicyclic polymers are conducive to threading with multiple linear chains[103]. Different from monocyclic polymers, multicyclic polymers demonstrate a much higher probability of ring bridging which is key to more effectively modulating mechanical properties[104]. As a result, the example PDMS network containing 60% (mass fraction) of mc-PDMS exhibits superior damping performance with a higher loss modulus.

4.3 Ring-ring Interlocked Structures

The ring-ring interlocked architecture embodies a distinctive topological motif *via* mechanical bonding at molecular scale, in which more than two independent closed-loop molecules are mutually penetrated to generate a chain-like interlocked configuration. The quintessential example of [n]catenane ($n\geq2$) as an inseparable mechanically interlocked structure consists of topologically entwined cyclic molecules without covalent linkage[92]. Catenanes display unique degrees of freedom covering elongation, twisting, and rotation[105]. The units are robust in the mechanical integrity by spatial entanglement although the covalent connections are absent.

Interlocked catenated poly(ε-caprolactone) (PCL) was synthesized *via* ring-expansion polymerization to achieve two mechanically interlocked polymers (MIPs) of $\overline{M}_n$=12000 and 22000 [Fig.11(A)][106]. DSC results show that the two polymers display the corresponding lower crystallinities of 42%—49% than the linear counterparts of 52%—57%, which originates from the constrained mobility imposed by the interlocked topology. WAXS results further indicate that the linear PCL sample could form a denser crystalline domain than MIPs [Fig.11(B)], implying that the structural restriction of entanglements is preserved permanently within the catenane framework. The mechanically linked polycarbonates (PCs) were synthesized by incorporating [2]catenane units *via* solid-state copolymerization[107]. Although the polymerization becomes heterogeneous by introducing the catenane at a high content, the glass transition temperature (T_g, ℃) is less influenced by the catenane moieties. This implies that the substantial internal motional freedom is well retained within the catenane structure which is greatly distinct from the rigid comonomers such as fluorene diol. Dynamic mechanical analysis (DMA) shows a transition at −6 ℃ in the copolymer film, which is attributed to the motion of either catenane ring or polymer segment [Fig.11(C)]. Even in the catenane-rich domains, polycarbonate chain dynamics remains decoupled from the catenane motions. A single metal-coordinated [2]catenane unit could be incorporated at the polymer mid-chain in MIPs [Fig.11(D)][108], where catenane flexibility is increased upon unlocking the macrocyclic entanglement after removal of palladium (Pd) ions to result in profound alterations in properties. While T_g is decreased in polystyrene after the Pd-decomplexation, crystallization in poly(ethylene oxide) (PEO) is greatly accelerated [Fig.11(E)]. This finding underscores the inherent correlation between enhanced motional freedom within catenane units and that of polymer chains.

Effective synthesis of polycatenane networks (Olympic gels) consisting of interlocked rings remains challenging [Fig.11(F)] although some unique performances have been predicted[92,109]. In nature, some topologies by interlocking DNA molecules are found[110]. DNA-based Olympic hydrogels by dynamic regulation

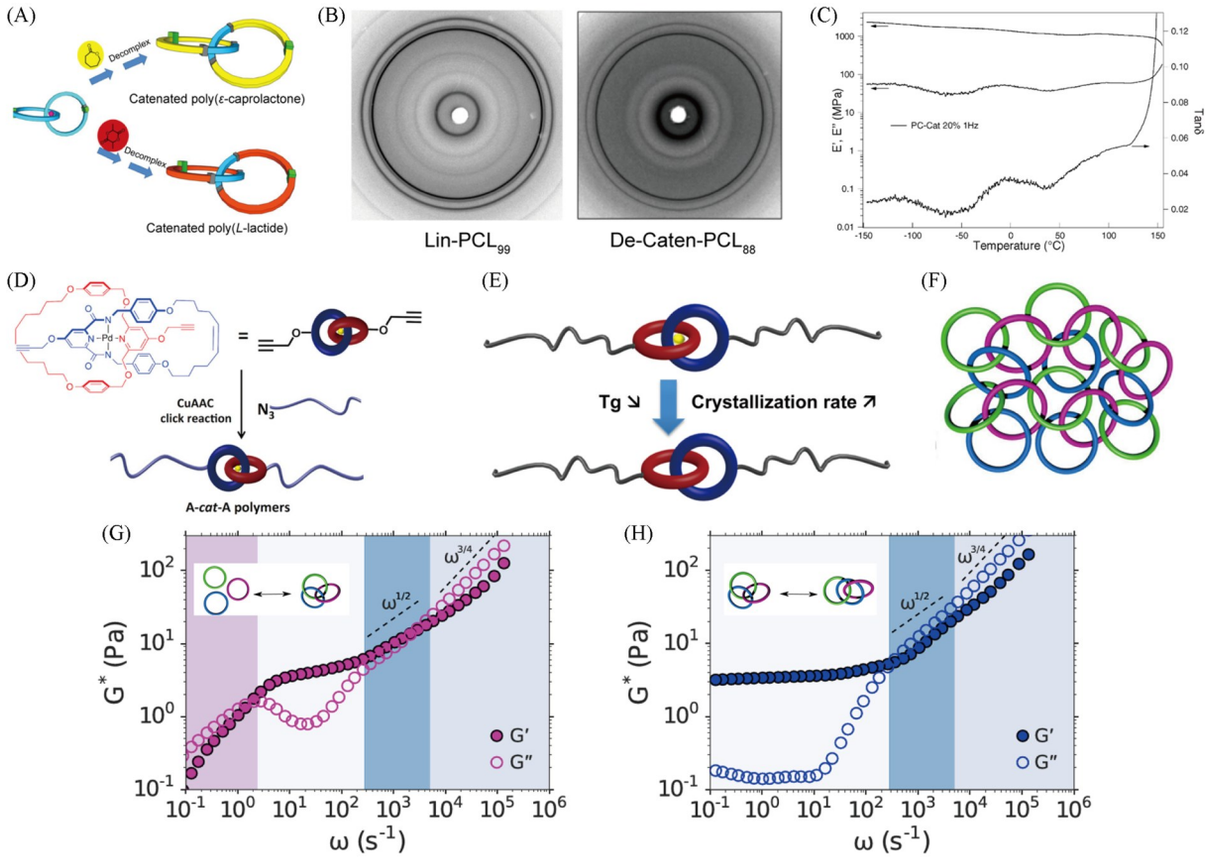

Fig. 11 Synthesis of the interlocked catenated poly(*ε*-caprolactone)(A), wide-angle *X*-ray scattering(WAXS) patterns of Lin-PCL$_{99}$ and De-Caten-PCL$_{88}$ crystals(B)[106], DMA spectra of the PC copolymer containing 20%(mass fraction) of [2]catenane(C)[107], synthesis of the catenane-based mechanically linked polymers (D) and Pd-removal of catenanes to enhance the polymer chain mobility, reduce T_g and increase crystallization rate(E)[108], schematic Olympic gel(F) and dynamic light-scattering microrheological behaviors of the enzyme-active gel(G) and permanent enzyme-inactive gel(H)[111]

(A, B) Copyright 2015, American Chemical Society; (C) Copyright 2003, American Chemical Society; (D, E) Copyright 2017, American Chemical Society; (F—H) Copyright 2018, American Physical Society.

with topoisomerases could be cleaved by enzymes and organized into DNA strands to facilitate mutual threading of circular DNA molecules. Introduction of topoisomerases to concentrated circular DNA solutions is necessary to promote the transient interpenetration and interlocking toward dynamic Olympic gels. After deactivating the enzymes, the interlocked network is permanently fixated by arresting strand cleavage and recombination[111]. Both dynamic(enzyme-active) and permanent(enzyme-inactive) gels exhibit elastic plateaus which is characteristic of an interlocked network at shorter timescales than enzymatic activity[Figs.11(G) and (H)]. Over extended durations, the dynamic gel experiences a fully relaxed stress akin to polymer solutions, whereas the permanent gel maintains solid-like elasticity. The enzymatic regulation enables reversible fluid-like and solid-like transition by controlling activity of the topoisomerase.

5 Summary and Outlook

Over the past several decades, large-scale synthesis of cyclic polymers has witnessed remarkable progress. The substantial breakthroughs in synthetic methodology by effective ring-closure are emergent at the infant stage, providing a powerful tool to fabricate highly pure polymer rings of tunable sizes, compositions and sequences. Both experiments and computations have elucidated the unique performances of polymer

rings. Especially, the viscoelastic behaviors could be finely tunable by precise control of the length, stiffness and microstructure of the polymer rings. The distinctive characteristics in mobility, viscoelasticity, and mechanical performances of the polymer rings render the flexible modulation of high performance nanomaterials. Rational design and easy processing of adaptive smart materials will become much easier. The programmable nanomaterials hold considerable promises in multidisciplinary fields such as energy storage, electronics, biomedicine, and aerospace exploration[112—117]. Despite the impressive strides achieved over the past decade, it remains challenging to extensively explore unique performances of the polymer rings and the functionalized nanocomposites toward engineering applications. The key issue remains focused on the development of facile and effective methods to large-scale fabrication of polymer rings of tunable sizes, compositions and microstructures. Analogous to linear polymers, control of sequence distribution of multi-compositions along the rings is pivotal, which is conducive to selective growth of desired functional materials at specific regions. Controllable conjugation of functional polymer single-chain at selective regions of the hybrid rings will provide a platform to integrate performances of polymers and nanoparticles toward functional superstructures. The hierarchically structured functional hybrid rings will be promising in large-scale fabrication of metamaterials which are responsive to external stimuli of such as optical, acoustic and electromagnetic fields. On the other hand, the hybrid rings would provide a new paradigm to drive the fast development of polymer science and engineering.

References

[1] Kricheldorf H. R., *J. Polym. Sci., Part A: Polym. Chem.*, **2010**, *48*(2), 251—284
[2] Hadziioannou G., Cotts P. M., ten Brinke G., Han G., Kovacs A., *Macromolecules*, **1987**, *20*(3), 493—497
[3] Kapnistos M., Lang M., Vlassopoulos D., Pyckhout-Hintzen W., Richter D., Cho D., Chang T., Rubinstein M., *Nat. Mater.*, **2008**, *7*(12), 997—1002
[4] Poelma J. E., Ono K., Miyajima D., Aida T., Satoh K., Hawker J., *ACS Nano*, **2012**, *6*(12), 10845—10854
[5] Córdova M. E., Lorenzo A. T., Müller A. J., Hoskins N., Grayson M., *Macromolecules*, **2011**, *44*(7), 1742—1746
[6] Zaldua N., Liénard R., Josse T., Zubitur M., Mugica A., Iturrospe A., Arbe A., de Winter J., Coulembier O., Müller J., *Macromolecules*, **2018**, *51*(5), 1718—1732
[7] Romio M., Trachsel L., Morgese G., Ramakrishna N., Spencer D., Benetti M., *ACS Macro Lett.*, **2020**, *9*(7), 1024—1033
[8] Golba B., Benetti E. M., de Geest B. G., *Biomaterials*, **2021**, *267*, 120468
[9] Xu X., Zhou N., Zhu J., Tu Y., Zhang Z., Cheng Z., Zhu X., *Macromol. Rapid Commun.*, **2010**, *31*(20), 1791—1797
[10] Morgese G., Cavalli E., Rosenboom J., Zenobi-Wong M., Benetti M., *Angew. Chem. Int. Ed.*, **2018**, *57*(6), 1621—1626
[11] Zhang K., Lackey M. A., Cui J., Tew N., *J. Am. Chem. Soc.*, **2011**, *133*(11), 4140—4148
[12] Aboudzadeh M. A., Iturrospe A., Arbe A., Grzelczak M., Barroso-Bujans F., *ACS Macro Lett.*, **2020**, *9*(11), 1604—1610
[13] Elardo M. J., Levenson A. M., Kitos V. A. P., Pomfret M. N., Golder M. R., *Chem. Sci.*, **2024**, *15*(41), 17193—17199
[14] Liu C., Cheu C., Barker J. G., Yang L., Nieh M., *J. Colloid Interf. Sci.*, **2023**, *630*, 629—637
[15] Martínez C. R., Pérez J. M., Arrabal-Campos F. M., Batuecas M., Ortuño M. A., Fernández I., *Polym. Chem.*, **2021**, *12*(28), 4083—4092
[16] Huo L., Qu K., Yang Z., Jia D., *Chin. J. Polym. Sci.*, **2025**, *43*, 399—405
[17] Guo X., Liu J. Y., Yang X. Y., Jin Z. L., Noritatsu T., *Chem. Res. Chinese Universities*, **2025**, *41*(4), 893—902
[18] Gao J. F., Lin X., Jiang B. W., Tang S. P., Zhang H. Y., Chen F. T., Jin Z. L., Li Y. J., Noritatsu T., *Chem. Res. Chinese Universities*, **2025**, *41*(4), 868—879
[19] Yan S. H., Wang L. J., Shan P. N., Lin X., Shi W. L., *Chem. Res. Chinese Universities*, **2025**, *41*(4), 859—867
[20] Guo D., Huang G. H., Bai H. J., Wang Y. L., Cao G. Q., Liu B., Hu S. L., *Chem. J. Chinese Universities*, **2025**, *46*(6), 20250091
[21] Liu S. Y., Su W., Zhou Z. Y., Yang Z. Y., Pei H. F., He Z. R., Wang N., Yue L., *Chem. J. Chinese Universities*, **2024**, *45*(11), 20240382
[22] Gao R., Xu L., Li S. Liu N., Chen Z., Wu Z., *Chem. Eur. J.*, **2023**, *29*(41), e202300916
[23] Ochs J., Pagnacco C., Barroso-Bujans F., *Prog. Polym. Sci.*, **2022**, 134, 101606
[24] Kricheldorf H., *Polycondensation: History and New Results*, Springer, Berlin, Heidelberg, **2014**
[25] Haque F., Grayson S., *Nat. Chem.*, **2020**, *12*(5), 433—444
[26] Hu J., Liu S., *Sci. China Chem.*, **2017**, *60*(9), 1153—1161
[27] Shao Y., Yang Z., *Prog. Polym. Sci.*, **2022**, 133, 101593

[28] Laurent B., Grayson S., *Chem. Soc. Rev.*, **2009**, *38*, 2202—2213
[29] Zhu Y., Hosmane N., *Chem. Open*, **2015**, *4*(4), 408—417
[30] Chang Y., Waymouth R., *J. Polym. Sci. Part A: Polym. Chem.*, **2017**, *55*(18), 2892—2902
[31] Ouchi M., Kammiyada H., Sawamoto M., *Polym. Chem.*, **2017**, *8*(34), 4970—4977
[32] Jia Z., Monteiro M., *J. Polym. Sci. A Polym. Chem.*, **2012**, *50*(11), 2085—2097
[33] Kricheldorf H., *Macromol. Symp.*, **2003**, *199*(1), 15—22
[34] Jacobson H., Stockmayer W., *J. Chem. Phys.*, **1950**, *18*(12), 1600—1606
[35] Josse T., DeWinter J., Gerbaux P., Coulembier O., *Angew. Chem. Int. Ed.*, **2016**, *55*(45), 13944—13958
[36] Hild G., Kohler A., Rempp P., *Eur. Polym. J.*, **1980**, *16*(6), 525—527
[37] Boutillier J., Lepoittevin B., Favier C., Masure M., Hémery P., Sigwalt P., *Eur. Polym. J.*, **2002**, *38*(2), 243—250
[38] Yin R., Hogen-Esch T., *Macromolecules*, **1993**, *26*(25), 6952—6957
[39] Iatrou H., Hadjichristidis N., Meier G., Frielinghaus H., Monkenbusch M., *Macromolecules*, **2002**, *35*(14), 5426—5437
[40] Madani A., Favier J., Hémery P., Sigwalt P., *Polym. Int.*, **1992**, *27*(4), 353—357
[41] Polymeropoulos G., Zapsas G., Ntetsikas K., Bilalis P., Gnanou Y., Hadjichristidis N., *Macromolecules*, **2017**, *50*(4), 1253—1290
[42] Blackburn S., Tillman E., *Macromol. Chem. Phys.*, **2015**, *216*(12), 1282—1290
[43] Konomoto T., Nakamura K., Yamamoto T., Tezuka Y., *Macromolecules*, **2019**, *52*(23), 9208—9219
[44] Sharma S., Ntetsikas K., Ladelta V., Bhaumik S., Hadjichristidis N., *Polym. Chem.*, **2021**, *12*(45), 6616—6625
[45] Zhang L., Wu Y., Li S., *Macromolecules*, **2020**, *53*(19), 8621—8630
[46] Qu L., Sun P., Wu Y., *Macromol. Rapid Commun.*, **2017**, *38*(15), 1700121
[47] Zhu X., Zhou N., Zhu J., Zhang Z., Zhang W., Cheng Z., Tu Y., Zhu X., *Macromol. Chem. Phys.*, **2013**, *214*(10), 1107—1113
[48] Sun P., Liu J., Zhang Z., Zhang K., *Polym. Chem.*, **2016**, *7*(12), 2239—2244
[49] Baeten E., Rubens M., Wuest K., Barner-Kowollik C., Junkers T., *React. Chem. Eng.*, **2017**, *2*(6), 826—829
[50] Chen L., Wang X., Hou R., Lu H., He Z., Zhou X., Zhang W., Wang X., *Polym. Chem.*, **2023**, *14*(40), 4659—4670
[51] Shen H., Wang G., *Polym. Chem.*, **2017**, *8*(36), 5554—5560
[52] Huettner N., Frisch H., Dargaville T., *Eur. Polym. J.*, **2024**, 203, 112659
[53] Ge Z., Zhou Y., Xu J., Liu H., Chen D., Liu S., *J. Am. Chem. Soc.*, **2009**, *131*(5), 1628—1629
[54] Liu Y., Jih J., Dai X., Bi G., Zhou Z., *Nature*, **2019**, *570*(7760), 257—261
[55] Zhang H., Zha H., Liu C., Hong C., *Sci. China Chem.*, **2022**, *65*(12), 2558—2566
[56] Zha H., Wang Z., Cheng L., Liu C., Hong C., *Macromolecules*, **2024**, *57*(24), 11322—11330
[57] Zha H., Wang Z., Liu C., Hong C., *Chin. Chem. Lett.*, **2024**, *35*(2), 108956
[58] Qu K., Du L., Zhou S., Huo L., Gu A., Lu D., Chen C., Di J., Yang Z., *Macromolecules*, **2025**, *58*(8), 4131—4137
[59] Golba B., Benetti E. M., de Geest B. G., *Biomaterials*, **2021**, *267*, 120468
[60] Peng L., Liu S., Feng A., Yuan J., *Mol. Pharm.*, **2017**, *14*(8), 2475—2486
[61] Park W. I., Kim Y., Jeong J. W., Kim K., Yoo J. K., Hur Y. H., Kim J. M., Thomas E. L., Alexander-Katz A., Jung Y. S., *Sci. Rep.*, **2013**, *3*(1), 3190
[62] Valero J., Pal N., Dhakal S., Walter N. G., Famulok M., *Nat. Nanotechnol.*, **2018**, *13*(6), 496—503
[63] Chen C., Weil T., *Nanoscale Horiz.*, **2022**, *7*(10), 1121—1135
[64] Kammiyada H., Ouchi M., Sawamoto M., *Macromolecules*, **2017**, *50*(3), 841—848
[65] Bielawski C. W., Benitez D., Grubbs R. H., *Science*, **2002**, *297*(5589), 2041—2044
[66] Halverson J. D., Grest G. S., Grosberg A. Y., Kremer K., *Phys. Rev. Lett.*, **2012**, *108*(3), 038301
[67] Jeong Y., Jin Y., Chang T., Uhlik F., Roovers J., *Macromolecules*, **2017**, *50*(19), 7770—7776
[68] Doi Y., Matsubara K., Ohta Y., Nakano T., Kawaguchi D., Takahashi Y., Takano A., Matsushita Y., *Macromolecules*, **2015**, *48*(9), 3140—3147
[69] Doi Y., Matsumoto A., Inoue T., Iwamoto T., Takano A., Matsushita Y., Takahashi Y., Watanabe H., *Rheol. Acta*, **2017**, *56*, 567—581
[70] Doi Y., *Nihon Reoroji Gakk.*, **2022**, *50*(1), 57—62
[71] Tsalikis D. G., Mavrantzas V. G., Vlassopoulos D., *ACS Macro Lett.*, **2016**, *5*(6), 755—760
[72] Parisi D., Costanzo S., Jeong Y., Ahn J., Chang T., Vlassopoulos D., Halverson J. D., Kremer K., Ge T., Rubinstein M., Grest G. S., Srinin W., Grosberg A. Y., *Macromolecules*, **2021**, *54*(6), 2811—2827
[73] Stano R., Smrek J., Likos C. N., *ACS Nano*, **2023**, *17*(21), 21369—21382
[74] Obukhov S. P., Rubinstein M., Duke T., *Phys. Rev. Lett.*, **1994**, *73*(9), 1263
[75] Kruteva M., Monkenbusch M., Allgaier J., Pyckhout-Hintzen W., Porcar L., Richter D., *Macromolecules*, **2023**, *56*(13), 4835—4844
[76] Yan Z., Wang W., *Macromolecules*, **2024**, *57*(9), 4236—4245
[77] Ge T., Panyukov S., Rubinstein M., *Macromolecules*, **2016**, *49*(2), 708—722
[78] O'Connor T. C., Ge T., Grest G. S., *J. Rheol.*, **2022**, *66*(1), 49—65
[79] O'Connor T. C., Ge T., Rubinstein M., Grest G. S., *Phys. Rev. Lett.*, **2020**, *124*(2), 027801
[80] Goto S., Kim K., Matubayasi N., *J. Chem. Phys.*, **2021**, *155*(12), 57—62

[81] Li Y., Wu Z., Zong Z., Cao X., *ACS Macro Lett.*, **2023**, *12*(2), 183—188
[82] Guo L., Wu C., Merlitz H., Chen J., Yang Z., Forest M. G., Wu C., Cao X., *Macromolecules*, **2025**, *58*(12), 6149—6157
[83] Chen D., Panyukov S., Sapir L., Rubinstein M., *ACS Macro Lett.*, **2023**, *12*(3), 362—368
[84] Xiong Z., Yu W., *Chin. J. Polym. Sci.*, **2023**, *41*(9), 1410—1424
[85] Minatti E., Viville P., Borsali R., Schappacher M., Deffieux A., Lazzaroni R., *Macromolecules*, **2003**, *36*(11), 4125—4133
[86] Honda S., Yamamoto T., Tezuka Y., *J. Am. Chem. Soc.*, **2010**, *132*(30), 10251—10253
[87] Poelma J. E., Ono K., Miyajima D., Aida T., Satoh K., Hawker C. J., *ACS Nano*, **2012**, *6*(12), 10845—10854
[88] Zhao D., Yan X., *Chem. Eur. J.*, **2025**, *31*(21), e202404780
[89] He L., Jiang Y., Wei J., Zhang Z., Hong T., Ren Z., Huang J., Huang F., Stang P. J., Li S., *Nat. Commun.*, **2024**, *15*(1), 3050
[90] Zhao D., Zhang Z., Wei Z., Zhao J., Li T., Yan X., *Angew. Chem. Int. Ed.*, **2024**, *63*(19), e202402394
[91] Xia D., Wang P., Ji X., Khashab N. M., Sessler J. L., Huang F., *Chem. Rev.*, **2020**, *120*(13), 6070—6123
[92] Hart L. F., Hertzog J. E., Rauscher P. M., Rawe B. W., Tranquilli M. M., Rowan S. J., *Nat. Rev. Mater.*, **2021**, *6*(6), 508—530
[93] Wang W., Bai R., Wang C., Yang L., Cheng L., Zhang Z., Yu W., Yan X., *Angew. Chem. Int. Ed.*, **2025**, *64*(30), e202507192
[94] Huang Z., Chen X., O'Neill S. J. K., Wu G., Whitaker D. J., Li J., McCune J. A., Scherman O. A., *Nat. Mater.*, **2022**, *21*(1), 103—109
[95] Wang L., Cheng L., Li G., Liu K., Zhang Z., Li, P., Dong S., Yu W., Huang F., Yan X., *J. Am. Chem. Soc.*, **2020**, *142*(4), 2051—2058
[96] Sawada J., Aoki D., Uchida S., Otsuka H., Takata T., *ACS Macro Lett.*, **2015**, *4*(5), 598—601
[97] Yang X., Cheng L., Zhang Z., Zhao J., Bai R., Guo Z., Yu W., Yan X., *Nat. Commun.*, **2022**, *13*(1), 6654
[98] Okumura Y., Ito K., *Adv. Mater.*, **2001**, *13*(7), 485—487
[99] Kato K., Yasuda T., Ito K., *Macromolecules*, **2013**, *46*(1), 310—316
[100] Mayumi K., Nagao M., Endo H., Osaka N., Shibayama M., Ito K., *Phys. Rev. B*, **2009**, *404*(17), 2600—2602
[101] Ito K., *Polym. J.*, **2012**, *44*(1), 38—41
[102] Ebe M., Soga A., Fujiwara K., Ree B. J., Marubayashi H., Hagita K., Imasaki A., Baba M., Yamamoto T., Tajima K., Deguchi T., Jinnai H., Isono T., Satoh T., *Angew. Chem. Int. Ed.*, **2023**, *62*(35), e202304493
[103] Hagita K., Murashima T., *Polymer*, **2021**, *223*, 123705
[104] Hagita K., Murashima T., Ebe M., Isono T., Satoh T., *Polymer*, **2022**, *245*, 124683
[105] Bai R., Zhang Z., Di W., Yang X., Zhao J., Ouyang H., Liu G., Zhang X., Cheng L., Cao Y., Yu W., Yan X., *J. Am. Chem. Soc.*, **2023**, *145*(16), 9011—9020
[106] Cao P. F., Mangadlao J. D., de Leon A., Su Z., Advincula R. C., *Macromolecules*, **2015**, *48*(12), 3825—3833
[107] Fustin C. A., Bailly C., Clarkson G. J., de Groote P., Galow T. H., Leigh D. A., Robertson D., Slawin A. M. Z., Wong J. K. Y., *J. Am. Chem. Soc.*, **2003**, *125*(8), 2200—2207
[108] Ahamed B. N., Van Velthem P., Robeyns K., Fustin C. A., *ACS Macro Lett.*, **2017**, *6*(4), 468—472
[109] Xiong X., Xue M., Xue L., Zhang L., Zhang Z., Chen J., Zhang G., Liu H., Cui J., *Angew. Chem. Int. Ed.*, **2025**, *64*(22), e202425034
[110] Renger H. C., Wolstenholme D. R., *J. Cell Biol.*, **1972**, *54*(2), 346—364
[111] Krajina B. A., Zhu A., Heilshorn S. C., Spakowitz A. J., *Phys. Rev. Lett.*, **2018**, *121*(14), 148001
[112] Wang J., O'Connor T. C., Grest G. S., Ge T., *Phys. Rev. Lett.*, **2022**, *128*(23), 237801
[113] Mo J., Wang J., Wang Z., Lu Y., An L., *Macromolecules*, **2022**, *55*(5), 1505—1514
[114] Bonato A., Marenduzzo D., Orlandini E., *Phys. Rev. Lett.*, **2025**, *134*(18), 188203
[115] Hagita K., Murashima T., *Macromolecules*, **2021**, *54*(17), 8043—8051
[116] Chiarantoni P., Micheletti C., *Macromolecules*, **2022**, *55*(11), 4523—4532
[117] Parisi D., Ahn J., Chang T., Vlassopoulos D., Rubinstein M., *Macromolecules*, **2020**, *53*(5), 1685—1693

(Ed.: W, K, M)